Sixth International Conference on Urban Earthquake Engineering
March 3-4, 2009, Tokyo Institute of Technology, Tokyo, Japan

LONG-PERIOD SITE RESPONSE IN THE TOKYO METROPOLITAN AREA

Kenichi Tsuda[1)], Takashi Hayakawa[1)], Kazuki Koketsu[2)], and Hiroe Miyake[3)]

1) Researcher, Center for Atomic Energy Engineering, Institute of Technology, Shimizu Corporation, Tokyo, Japan
2) Professor, Earthquake Research Institute, University of Tokyo, Tokyo, Japan
3) Assistant Professor, Earthquake Research Institute, University of Tokyo, Tokyo, Japan
kenichi.tsuda@shimz.co.jp, takashi.hayakawa@shimz.co.jp, koketsu@eri.u-tokyo.ac.jp, hiroe@eri.u-tokyo.ac.jp

Abstract: We have derived the spatial variation of site response for the greater Tokyo metropolitan area in the long -period range of 2 to 4 s. The site responses have been obtained by the spectral inversion method developed by Tsuda *et al.* (2006). The general features of spatial variation of site response roughly correlate with the surface geology classification by Wakamatsu and Matsuoka (2006). The effect of focal mechanism on site response is included, because the site responses estimated at three KiK-net stations with this effect is closer to the observed one than the site responses estimated without this effects. In particular, site responses near nodes or lobes of the radiation pattern are much affected by this effect. Our results indicate that the geometrical relation of a target site to the seismic source is important for the site response estimation and the inclusion of focal mechanism effect can lead to more realistic ground motion predictions for a specific scenario event.

1. INTRODUCTION

The observed ground motions are constituted by three different factors: seismic source (source effects), wave propagation through heterogeneous earth's interior (path effects), and local geological conditions (site effects). This relationship can be represented by the following equation;

$$O(t) = S(t) * P(t) * G(t) \qquad (1)$$

where * is the convolution operator, O(t) is the observed records, S(t) means the source effects of earthquake ruptures, P(t) means the path effects of wave propagation through the heterogeneous earth's interior, and G(t) means the site response close to the stations. This basic equation has been used to estimate site response based on the observed records.

Among those three effects, site response plays an important role for the ground motion prediction since Reid (1910) pointed out that the level of ground motion correlates with the type of surface geology. Previously, estimation of site response for the period of 0.1-2 s was important, because the number of low-profile buildings with 0.2-0.5 s resonant period was much large compared to large scale structures such as high-rise buildings, oil storage tanks, and base-isolated building *etc.* with usually longer resonant period (1 s or longer). However, increasing number of such large scale structures (e.g., Fukuwa and Tobita, 2008) leads to the recognition of the importance of spatial variation of site response for a long-period range.

In addition to the increasing of such large scale structures, the Tokyo metropolitan area has a very high possibility to have the large earthquakes that can produce very damaging long-period ground motions in near future (The Headquarters for Earthquake Research Promotion, 2007). Such large events can produce the near-source long period ground motions (Koketsu and Miyake, 2008) as well. This means that estimation of site response for longer period in order to predict the long-period ground motions for future earthquakes is an urgent task.

In this study, the site responses for a long-period range (longer than 1 s) have been estimated by using the spectral inversion method (Tsuda *et al.*, 2006). Since this method is reference-independent, site response from the seismological basement to the surface might be estimated. Because some previous studies showed the effects of focal mechanism on the observed ground motions in a long-period range, we have taken into account the effects of focal mechanism into site response estimation. We have used the data recorded at the Tokyo metropolitan area where there are more than 800 strong motion sites. After we obtain site response on all the sites, we have investigated the spatial variation of site response.

2. DATA

We have used the observed data collected by the Seismic Kanto Strong motion-network (SK-net), K-NET and KiK-net. The SK-net began operation after the 1995 Kobe earthquakes for the purpose of seismic hazard mitigation around the Kanto area. This array consists of three-component accelerometers for more than 800 surface

stations and more than 70 borehole stations (Seismic Kanto Research Project, 2001). For this study, we selected 19 events that occurred around the Kanto area. Each event was recorded on almost all of the KiK-net borehole accelerographs as well as most surface stations (Table 1). The epicenters, shown as solid red circles, and the station distribution are shown in Figure 2. The solid blue triangles denote the stations used to determine source and path parameters. The focal depths are greater than 50 km; magnitudes range between 4.5-5.8. Average hypocentral distances to the array vary from 50 to 130 km (Figure 1). In Table 1, we give the source location, focal depth and magnitude determined by the F-net/NIED for each event. We also show the source parameters (seismic moment: *Mo*, and corner frequency: *fc*) in the same table.

Table 1: List of earthquakes used in this study. Mo and fc denote the estimated seismic moments and corner frequencies by Tsuda *et al.* (2008): Mo (NIED) is those determined by F-net/NIED (Fukuyama *et al.*, 1998).

	Event (Date)	Lat.† (N)	Long.† (E)	Depth† (km)	Mw	Moment† [Nm]	Moment§ [Nm]	fc§ [Hz]
1	3/13/03	36.09	139.87	50	4.9	2.34E+16	2.41E+16	1.95
2	4/8/2003	36.07	139.91	44	4.8	2.11E+16	1.58E+16	1.69
3	5/10/2003	35.81	140.11	65	4.7	1.37E+16	2.00E+16	1.41
4	5/12/2003	35.87	140.09	50	5.2	7.07E+16	3.87E+16	1.28
5	5/17/03	35.74	140.7	53	5.3	1.13E+17	1.03E+17	0.71
6	8/18/03	35.8	140.11	71	4.8	1.92E+16	2.55E+16	1.55
7	9/20/03	35.22	140.3	56	5.7	3.53E+17	2.22E+17	0.89
8	10/15/03	35.61	140.05	68	5.1	5.15E+16	5.32E+16	1.60
9	7/10/04	36.08	139.89	50	4.7	1.21E+16	1.34E+16	2.10
10	7/17/04	34.83	140.36	59	5.6	2.39E+17	1.40E+17	1.34
11	8/6/04	35.61	140.06	71	4.7	1.27E+16	1.92E+16	1.98
12	10/6/04	35.99	140.09	65	5.7	4.52E+17	2.80E+17	0.78
13	2/8/05	36.14	140.09	65	4.9	2.20E+16	1.88E+16	2.11
14	2/16/05	36.04	139.9	53	5.4	1.33E+17	7.44E+16	1.52
15	4/10/05	35.73	140.62	50	5.8	4.95E+17	5.52E+17	0.42
16	6/20/05	35.73	140.69	51	5.5	1.94E+17	1.26E+17	0.81
17	7/23/05	35.58	140.14	73	4.7	4.74E+17	4.64E+17	0.84
18	7/28/05	36.13	139.85	51	4.7	1.17E+16	9.58E+15	3.00
19	8/7/05	35.56	140.11	73	4.5	6.88E+15	1.30E+16	2.35

†These parameters were determined by National Institute for Earth Science and Disaster Prevention (NIED), Tsukuba, Japan.

§ Resultant source paramters

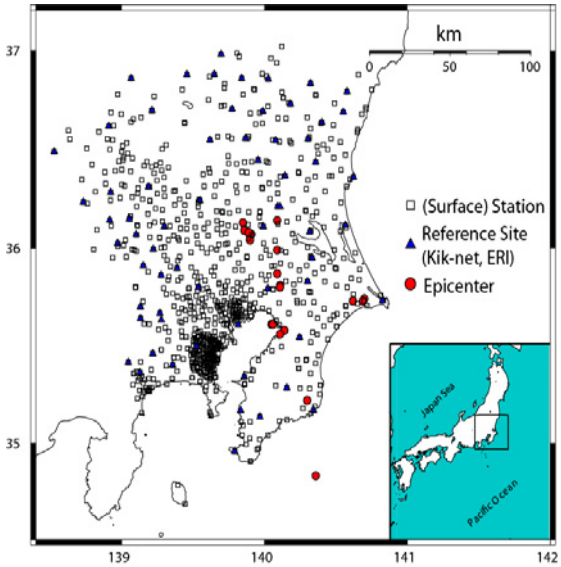

Figure 1: Geography of the Kanto region. Epicenters of the events listed in the Table 1 are plotted in map view by solid circles. Solid triangles colored by blue denote the reference station used to determined source and path parameters by Tsuda *et al.* (2008). Open squares mean the surface stations used in this study.

For our analysis, we used the two horizontal components at each site. A 10 s time window beginning 1.0 sec before the first *S*-wave arrival was picked for all events. We applied a cosine window taper of 0.5 sec to both ends of the record. After the Fourier amplitude spectrum of each component was calculated, we used vector summation of the two horizontal components as the amplitude spectrum. During checking the observed data, we eliminated the data including noise in longer period range.

3. ESTIMATING SITE RESPONSE

3.1 Spectral Inversion Analysis

In order to estimate site response, we have to separate the source and path effects from observed records. We have applied the spectral inversion analysis developed by Tsuda *et al.* (2006) to separate these three factors. Tsuda *et al.* (2008) applied this method to estimate site response in the Tokyo metropolitan area for a period range of 0.1-2 s. Then we have derived the site response for a period range of 2-4 s.

Explaining the detail concept for the spectral inversion analysis is found on many articles (Iwata and Irikura, 1988; Bonilla *et al.*, 1997; Yamanaka *et al.*, 1998; Satoh *et al.*, 2001) and is beyond this study, we show the brief introduction of this method.

The observed ground motion for linear response—can be expressed as a convolution of the source, path, and site (Eq1). In a frequency domain, this equation can be rewritten as a multiplication:

$$|A(f)| = |S(f)|\,|Site(f)|\,R^{-1}\,e^{-\pi f R / Q(f)\beta} \qquad (2)$$

where f is frequency, $|A(f)|$ is the acceleration amplitude spectrum of the recorded ground motion, $|S(f)|$ is the source spectrum, $Q(f)$ is the quality factor, which is assumed to be frequency dependent, $|Site(f)|$ is the site response amplitude, R is the distance from source (Table 1) to site, and β is the average shear wave velocity of the medium (3.7 km/s, Yamanaka *et al.*, 1998). To estimate the site response, it is necessary to isolate these three factors from observed records. In general, isolating each element requires constraints to avoid tradeoffs among these three elements. A standard constraint is to impose a condition on a rock station. Another approach is to define a source spectrum for a specific 'reference' event. Because some shallow borehole records (reference station) may be contaminated the borehole response itself, we used a method to separate the source, path and site effect that is independent of a reference station (Tsuda *et al.*, 2006).

Equation 3 uses Boatwright's (1978) representation of a source spectrum (Brune, 1970), in which the amplitude of the source spectrum has a nonlinear dependence on the corner frequency:

$$|S(f)| = C\, M_o (2\pi f)^2 \cdot f_c^2 / (f^4 + f_c^4)^{0.5} \qquad (3)$$

where

$$C = (G_0 \cdot F^{rad}) / (4\pi\rho V_S^3) \qquad (4)$$

C depends on the radiation parameter of the source: F^{rad} is the effects of this radiation pattern coefficients on site response estimation will be discussed, the material parameters for source area (3000 [kg/m³] for density: ρ and 4.5 [km/sec] for shear wave velocity: V_S) and the free surface effect G_o is included. We assumed that the radiation pattern coefficient F^{rad} is frequency-independent. The seismic moment M_o and corner frequency f_c are determined from the spectrum (Brune, 1970). We show the source parameters estimated by Tsuda *et al.* (2008) in Table 1 and Figure 2. The resultant seismic moments agree with the values determined by F-net/NIED (Figure 2 (a)), and calculated stress drop based on the resultant corner frequency (Figure 2 (b)) follows the previous studies (Brune, 1970). These indicate that their estimates for source parameters are reasonable. We have used these parameters to estimate source spectrum based on Eq (3).

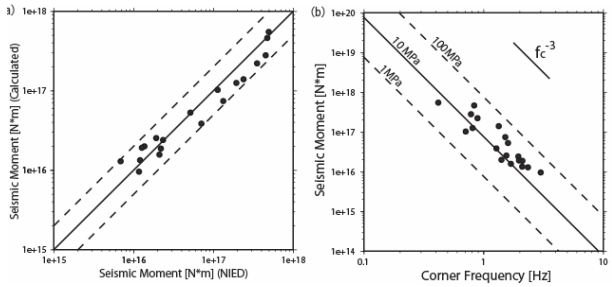

Figure 2: (a) Seismic moments from Tsuda *et al.* (2008) are compared with those from F-net/NIED. Dashed lines show a factor of two. (b) Seismic moment is plotted versus corner frequency for the 19 events. Lines of constant stress drops (Brune) are plotted. Within a factor of two the stress drops are ~10 MPa.

Including the path effect introduces a nonlinear dependence on frequency when the attenuation parameter $Q(f)$ is assumed to have a power law dependence on frequency: $Q(f)=Q_o f^{\prime}$. In this study, we have used the $Q(f) =107 f^{0.52}$ derived by Tsuda *et al.* (2008). This model agrees with the other models derived for this area.

3.2 Estimating Site Response

Importance of Radiation Pattern: After having the source effects for each events and path effect, we have derived the site response for 2-4 s. Compared to the site response for the short period range, the source effects such as the focal mechanism in a long-period (2-4 s) ground motions for site response are getting pronounced (Kamae *et al.*, 1990). We have calculated the RMS of vector amplitude normalized by the maximum values for *S*-wave for a 2-4 s period range at each site. We show the spatial distribution of RMS peak ground velocity vectors and radiation pattern coefficients as the examples in Figure 3. The radiation pattern coefficient is getting very small when the geometrical relation of the site to the source is located on the nodes (blue-shaded area). On the other hand, the coefficient is very large when its geometrical relation is located on the lobes (red-shaded area). As we show the figures, the difference of two cases (lobes and nodes) can be the factor of 3. This suggests that we need to the effects of focal mechanism on the estimation of site response in a long-period range (2-4 s).

Site Response Estimation with Focal Mechanism: In this study, we have incorporated the effects of focal mechanism into estimating site response. We calculated the radiation coefficients (Aki and Richards, 2002) for each record based on the mechanism determined by F-net/NIED (Fukuyama *et al.*, 1998) and substitute it into Eq 4. After we calculate source spectrum (Eq 3), the site response has been derived by using $Q(f)$. We averaged the site response calculated for each event. We show the contour map of site response for 2-4 s in Figure 4(a). The general feature of spatial variation of site response looks similar to the site response map based on the classification of surface geology (Wakamatsu and Matsuoka, 2006), i.e. the region of very weak soil like swanpy area, shown in the Figure 4(b) has large site response.

In Figure 5, we have compared the predominant periods of our resultant site response and those from H/V ratios of microtremor measurements at K-NET sites (Tanaka *et al.*, 2005). We plotted the predominant periods from only sites with apparent ones, because the apparent predominant periods of H/V ratio clearly agree with the site response estimates from other methods, such as spectral inversion method, spectral amplitude ratio *etc* (Bonilla *et al.*, 1997; Satoh *et al.*, 2001). Thus, we picked these sites based on the criteria that the difference between peak and trough of site response function is more than 50%. As shown in the figure, the predominant periods from our resultant site responses agree with H/V ratios, indicating that our estimates of site response are reasonable.

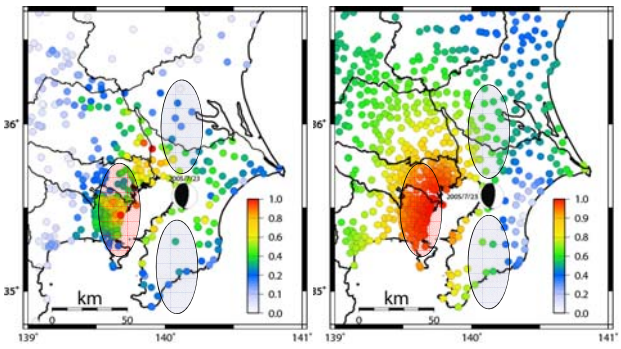

Figure 3: Distribution of normalized RMS observed peak ground velocity vectors for the event 17 (2005/7/23). Each value is the hypocentral distance corrected values at R =100 km (left). Spatial variation of radiation pattern coefficients of the same event for all sites (right).The focal mechanism has been determined by F-net/NIED.

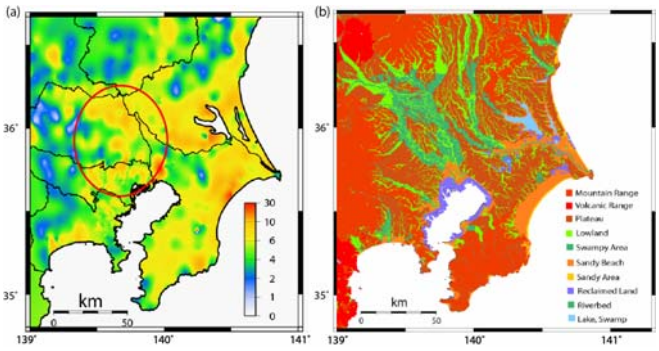

Figure 4: Spatial distribution of site response for a period range of 2-4 s (a). The area with large site response values (around red circle of left figure) correspond to the very weak surface geology, such as swanpy area classified by Wakamatsu and Matsuoka (2006) (b).

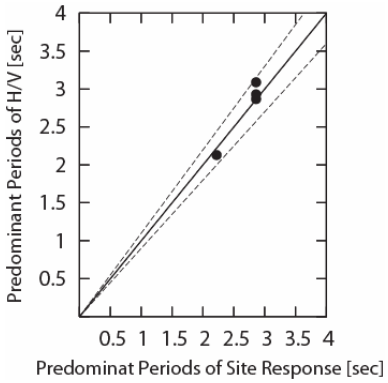

Figure 5: Comparison of predominant period of site response estimates. The solid line denotes the equal values of predominant periods.

4. DISCUSSION

The difference of site response between two cases for different F^{rad} (theoretical radiation and isotropic radiation) is discussed in this chapter. The derived site response in this study includes the effects of focal mechanism. This means that the theoretical radiation of seismic wave is assumed. However, the isotropic radiation (F^{rad} in Eq 4 is set to be 0.63, Boore and Boatwright, 1984) of seismic wave is usually assumed for the estimation of site response in short period range and the necessity of incorporation of the effects of focal mechanism into site response estimation is not clear yet in long period range. We calculated the site response with assuming isotropic radiation and show the spatial variation in Figure 6 (right). As we compare the results of theoretical radiation (Figure 6, left), the general features of spatial variation of site response is very similar. However, if we take the ratio of these two values, the hatched area in Figure 7 has some differences between two site responses. Because this area corresponds to the node of theoretical radiation based on the geometrical relation for many events (Figure 1), site responses tends to be large (radiation pattern coefficients in Eq 4 becomes small) compared to the other area.

In order to examine the effects of radiation pattern on site response as well as to validate our results, we compared our results with observed spectral amplitude ratio (surface / borehole) on some KiK-net sites. We picked three sites inside the Kanto basin (locations are also shown in Figure 7) that their borehole depth is "close" to the seismological basement *i.e.*, the *S*-wave velocity of borehole depth is close to 3.0 [km/sec]. Also their location is close to the area with big difference of site response (radiation pattern coefficients). However, because the definitions of our resultant site response corresponds to the ratio from the seismological basements (not borehole depth) to the surface, correction of the observed spectral ratio: $R_o(f)$ (surface/borehole) is necessary. The correction is based on the ratio of material impedance as follows (Shearer, 1999)

$$R_C(f) = (\rho_1\beta_1 / \rho_2\beta_2)^{0.5} \cdot R_o(f) \qquad (5)$$

where ρ_i, β_i, are the material properties (density and shear wave velocity) of seismological basement (i=1) and borehole depth (i=2).

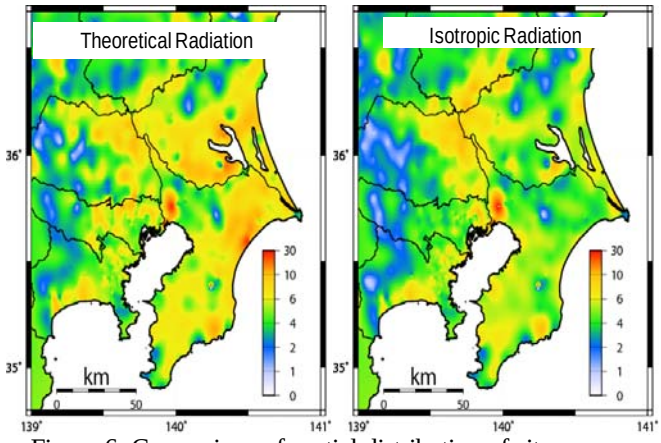

Figure 6: Comparison of spatial distribution of site response between theoretical radiation (left) and isotropic radiation (right) for a period range of 2-4 s.

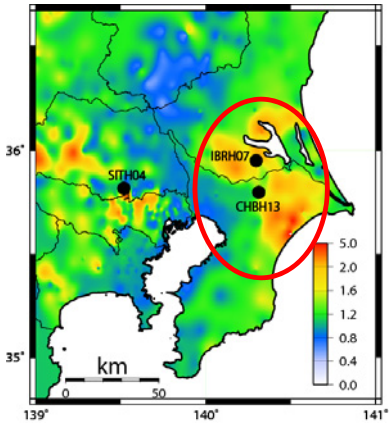

Figure 7: Spatial variation of site response ratio (theoretical radiation / isotropic radiation) for a period range of 2-4 s.

We used the values of material property at the borehole depth given by NIED and the generic values at the seismological basement (ρ = 2.9, β = 3.7 [km/sec]) based on previous studies (e.g. Tsuda et al., 2008; Ludwig *et al.*, 1970) are assumed. In Figure 8, we show the comparison of our site response (red curve for theoretical radiation and green curve for the isotropic radiation) and corrected site response (blue curve). As shown for all sites, the site response based on theoretical radiation (red line) is getting closer to the corrected observed spectral ratio (blue line) for the frequency range of 0.25 Hz (4 sec) - 0.5 Hz (2 sec). This indicates that modeling site response including the effects of radiation pattern might lead to the better estimation of site response at site that their geometrical relation is node (or lobe) of theoretical radiation.

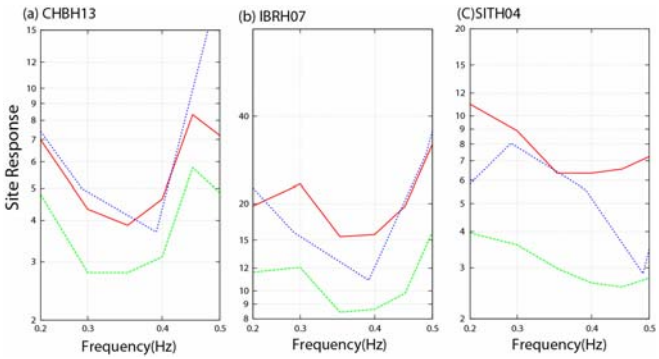

Figure 8: Comparison of site response for theoretical radiation (red), isotropic radiation (green), and corrected observed spectral ratio (blue) at three KiK-net sites.

5. SUMMARY

In this study, we have derived the long-period (2-4 s) site response with the effects of focal mechanism. The agreement of spatial variation of observed values of RMS of vector amplitudes for 2-4 s *S*-wave with of radiation coefficients suggest the necessity of incorporation of focal mechanism into the estimation of site response. The general features of spatial variation of site response agree with the other studies based on the classification of surface geology. Also the predominant periods of our site responses agree well with those from H/V ratios of microtremor, indicating that our estimates of site response are reasonable.

Our resultant site responses with considering the effects of focal mechanism are closer to the observed spectral ratio corrected based on the material impedance ratio. This indicates that modeling site response including the effects of radiation pattern might lead to the better estimation of site response in a long-period range. Incorporating the effect of complex velocity structure beneath the Kanto area on ray paths into estimating site response and our results into developing velocity model might be the next steps. The development of velocity model leads to the better understandings of ground motion complexity and is useful for the ground motion prediction for the future large disastrous events (e.g., Sekiguchi *et al.*, 2008).

Acknowledgements:

We thank to Prof. Saruboh Midorikawa for his invitations. Creating some figures is helped by Mr. N. Matsui from Esco Corporation.

References:

Aki, K. and P. Richards. (2002). Quantitative Seismology, 2nd edition, University Science Books.

Boatwright, J. (1978). Detailed spectral analysis of two small New York State earthquakes, *Bull. Seism. Soc. Am.* **68,** 1117-1131.

Bonilla, L.F., J. H. Steidl, G. T. Lindley, A. G. Tumarkin, and R. J. Archuleta (1997). Site amplification in the San Fernando valley, California: variability of site-effect estimation using the S-wave, coda, and H/V methods, *Bull. Seism. Soc. Am.* **87**, 710-730.

Boore, D. M., and J. Boatwright. (1984). Average body-wave radiation coefficient, *Bull .Seism. Soc. Am.* **74**, 1615-1621.

Borcherdt, R.D. (1970). Effects of local geology on ground motion near San Francisco Bay, *Bull. Seism. Soc. Am.* **60**, 29-61.

Brune, J. N. (1970). Tectonic stress and the spectra of seismic shear waves from earthquakes, *J. Geophys. Res*, **75,** 4997-5009.

Fukuyama, E., M. Ishida, D. S. Dreger, and H. Kawai (1998). Automated seismic moment tensor determination by using on-line broadband seismic waveforms, *Zisin.* **51**, 149-156. (Japanese with English abstract)

Fukuwa, N., and J. Tobita (2008), Key parameters governing the dynamic response of long-period structures, *J. Seismol*., **12**, 295-306.

Iwata, T., and K. Irikura. (1988). Source parameters of the 1983 Japan Sea earthquake sequence, *J. Phys. Earth*. **36**, 155-184.

Kamae, K., K. Irikura, and Y. Fukuchi (1990), Prediction of strong ground motion for M7 earthquake using regional scaling relations of source parameters, *J. Struct. Constr. Eng.* **416,** 57–70 (Japanese with English abstract).

Koketsu, K., and H. Miyake (2008), A seismological overview of long-period ground motion, *J. Seismol.*, **12**, 133-143.

Ludwig, W. J., J.E. Nafe, and C. L. Drake (1970), "Seismic refraction", *The Sea*, **4**, 53-84.

Mai, M. (2007), Ground Motion: Complexity and scaling in the near field of earthquake ruptures

Reid, H. F. (1910). The California earthquake of April 18, 1906, Publication 87, V21, Carnegie Institute of Washington, Washington, D.C.

Seismic Kanto Research Project, Earthquake Research Instiutute, University of Tokyo. (2001), http://www.sknet.eri.u-tokyo.ac.jp/ (in Japanese).

Satoh, T., H. Kawase, and S. Matsushima (2001), Differences between site characteristics obtained from microtremors, S-waves, P-waves, and codas, *Bull. Seism. Soc. Am.* **91,** 313-334.

Sekiguchi, H., H. Horikawa, and M. Yoshimi (2008), Broadband ground motion prediction in Kanto basin due to hypothetical Kanto earthquakes, Programme and Abstracts, The 7th General Assembly of Asian Seismological Commission.

Shearer, P. (1999). "Introduction to Seismology", Cambridge University Press.

Tanaka, Y., K. Koketsu, H. Miyake, T. Furumura, H. Sato, N. Hirata, H. Suzuki, and T. Masuda (2005), Integrated modeling of 3D velocity structure beneath the Tokyo metropolitan area, *EOS Trans*, AGU, 86(52), Fall Meeting Suppl, Abstract S21A-0200.

The Headquarters for Earthquake Research Promotion (2007) Report ' National Seismic Hazard Maps for Japan

Tsuda, K, Y. Hisada, and K. Koketsu (2008). Estimation of site

response for Kanto Plain by use of the data from dense strong motion seismograph array, in preparation to *Bull. Seism. Soc. Am.*

Tsuda, K., Archuleta, R., and Koketsu, K. (2006). Quantifying spatial distribution of site response by use of the Yokohama High-Density Strong Motion Network, *Bull. Seism. Soc. Am.* **96,** 926-942.

Yamanaka, H., A. Nakamaru., K. Kurita., and K. Seo. (1998). Evaluation of site effects by an inversion of S-wave spectra with a constraint condition considering effects of shallow weathered layers, *Zisin* **51,**193-202 (in Japanese with English abstract).

Wakamatsu, K., and M. Matsuoka. (2006). Development of the 7.5-arc-second engineering geomorphologic classification database and its application to seismic microzoning, *Bull. Earthq. Res. Inst.* **81**, 317-324.